www.editada.org

International Journal of Combinatorial Optimization Problems and Informatics, 18(1), 2027, 87-100. ISSN: 2007-1558.
https://doi.org/10.61467/2007.1558.2027.v18i1.1494

Real-Time Discrete PID Control of a Low-Cost, Open-Hardware Inverted Pendulum on a Cart: Design, Construction, and Experimental Validation

Víctor Alexis Hernández Rios[1], José Manuel Franco Rivera[1], Emmanuel Martínez Ramirez[1], Evelin Gutiérrez Moreno[2], Amadeo Manuel Hernández Hernández[1], Javier Hernández Pérez[2]

[1]Departamento de Ingeniería Eléctrica y Electrónica, Tecnológico Nacional de Mexico, Campus Pachuca, Mexico.

[2]Departamento de Ingeniería Mecatrónica, Universidad Politécnica de Pachuca, Mexico.

l23200076@pachuca.tecnm.mx, l23200242@pachuca.tecnm.mx, l22200604@pachuca.tecnm.mx, evgutierrez@upp.edu.mx, amadeo.hh@pachuca.tecnm.mx, jahdez@upp.edu.mx

Abstract. This work presents the design, construction, and experimental validation of a low-cost inverted pendulum on a cart as an open-hardware didactic platform for control education. The non-linear, underactuated, and inherently unstable dynamics were derived via the Euler-Lagrange formulation and linearized about the unstable equilibrium to obtain a continuous-time model, subsequently discretized into a digital Proportional-Integral-Derivative (PID) control law implemented on an 8-bit Arduino-bazed microcontroller. Feedback was obtained from two quadrature encoders, while actuation was provided through an H-bridge-driven DC motor. Two empirically tuned gain sets were evaluated: an aggressive configuration achieved clozed-loop stabilisation within 33 seconds despite increazed mechanical vibration, whereas a conservative configuration proved insufficient, yielding a sustained oscillatory limit cycle. These results confirm that classical PID control, tuned experimentally, can compensate for unmodelled phenomena such as friction, actuator dead zones, and backlash. At under US$112, the prototype offers a reproducible, accessible alternative to commercial control engineering laboratory equipment.

Keywords: Inverted pendulum on a cart, underactuated systems, discrete-time PID control, open-hardware embedded platform, experimental tuning

Article Info
Received: Jun 21, 2026
Accepted: Aug 01, 2026

1. Introduction

The inverted pendulum mounted on a cart constitutes one of the most widely studied benchmark systems in nonlinear control theory, owing to its combination of underactuation, open-loop instability, and non-minimum-phase dynamics (Aracil & Gordillo, 2005). Because the number of independent actuators is smaller than the number of degrees of freedom, a single horizontal force applied to the cart must simultaneously regulate two coupled coordinates: the linear displacement of the cart and the angular position of the pendulum about its unstable upright equilibrium. Aracil and Gordillo (2005) characterized this configuration as posing a twofold control problem, local stabilisation in the neighbourhood of the unstable equilibrium, and global manoeuvring capable of driving the pendulum from rest to that equilibrium, establishing the platform as a paradigmatic testbed against which nonlinear and optimal control strategies continue to be validated.

Beyond its theoretical relevance, the inverted pendulum raises a genuinely computational question: how can a controller capable of stabilising a fast, strongly coupled, inherently unstable plant be executed deterministically, in real time, on processing hardware with limited computational and memory resources? This question remains unresolved in the literature" o "This question has not been fully addreszed in the literature. Several recent studies have pursued increasingly sophisticated algorithmic solutions. Lomeli (2025) demonstrated that polynomial neural networks can yield accurate parametric approximations of nonlinear plant dynamics, offering a data-driven alternative to analytical modelling. Juárez-Lora and Hernández-Pérez (2022) implemented a Linear Quadratic Regulator using spiking neural networks for underactuated systems, illustrating how neuromorphic computation can be embedded within optimal control architectures. Hernández-Pérez and Gutiérrez (2024) extended LQR-based control with gravity compensation to a turbine-pendulum system, showing that pendulum-derived control architectures generalise to large-scale industrial applications such as wind-turbine blade dynamics. Alvarado-Hernández et al. (2025) and Narciso et al. (2023) combined fuzzy PID control with state estimation to stabilise an aero-pendulum, confirming that hybrid intelligent strategies remain competitive even for classical electromechanical benchmarks.

Despite these algorithmic advances, the literature consistently identifies a persistent and largely unresolved obstacle: the transition from a controller validated in simulation to one operating reliably on physical, resource-constrained hardware. Digital simulation environments support stability analysis and preliminary tuning but routinely neglect friction, mechanical backlash, actuator dead zones, sensor quantisation, and the finite execution time available within a fixed sampling period. Closing this gap requires not only a correct mathematical model but also an embedded software architecture capable of meeting strict real-time constraints, interrupt-driven sensor acquisition, deterministic control-loop execution, and digital filtering, within the limited memory and clock speed of low-cost microcontrollers.

A second, closely related barrier is economic. Specialized commercial platforms for control engineering education routinely cost several thousand US dollars, restricting hands-on access to underactuated, unstable systems in many university laboratories. This barrier has motivated a growing body of work on open-hardware didactic prototypes. Medina Cervantes et al. (2017) demonstrated, with an early Furuta pendulum prototype, that physical interaction with an underactuated system provides pedagogical value that purely simulated exercises cannot replicate. Martínez Ramírez and Hernández Hernández (2025) subsequently developed a low-cost educational Furuta pendulum, confirming that open-hardware components can reproduce the dynamic richness of commercial rotary pendulum platforms at a fraction of the cost. Yanco Melgarejo (2026) advanced this line further by implementing a clozed-loop digital PID controller augmented with Kalman filtering for sensor-noise reduction on an Arduino Mega platform, stabilizing a low-cost aerodynamic pendulum using control logic implemented entirely within an 8-bit embedded architecture, directly demonstrating that deterministic, noise-robust control execution is achievable on resource-constrained hardware.

Taken together, this body of work indicates that, whilst advanced algorithms increasingly dominate the theoretical literature, the cart-mounted inverted pendulum configuration, as distinct from the Furuta and aero-pendulum variants already addreszed, has received comparatively little attention from an embedded, real-time, low-cost computational perspective. The scientific question motivating the present work is therefore the following: can a deterministic, discrete-time control law be designed, discretized, and executed in real time on an 8-bit, resource-constrained microcontroller to stabilise the nonlinear, underactuated, unstable dynamics of an inverted pendulum on a cart, using an open-hardware platform reproducible at low cost?

To address this question, the present work proposes the design, construction, and experimental validation of a low-cost, open-hardware inverted pendulum on a cart. The nonlinear equations of motion are derived using the Euler-Lagrange formulation and linearized about the unstable upright equilibrium to obtain a continuous-time state model. This model underpins a continuous Proportional-Integral-Derivative control law, which is subsequently discretized, via backward-difference differentiation and trapezoidal integration, into a velocity-form difference equation suitable for deterministic execution within a fixed sampling period. The resulting controller is implemented on an 8-bit ATmega328P microcontroller, with feedback provided by two quadrature optical encoders acquired through hardware interrupts, derivative low-pass filtering to suppress quantisation noise, integral anti-windup saturation, and actuation delivered via an H-bridge-driven direct-current motor.

It is hypothesized that, despite its conceptual simplicity relative to the optimal and intelligent control strategies reviewed above, a classical discrete-time PID controller, tuned empirically rather than through model-bazed optimisation, can achieve effective real-time stabilisation of the inherently unstable pendulum-cart system on resource-constrained embedded hardware, provided that the gains are adjusted to compensate for unmodelled physical nonlinearities such as static and dynamic friction, mechanical backlash, and actuator dead zones that digital simulation alone cannot capture.

The principal contribution of this work is threefold. First, it provides a complete, reproducible methodological pathway, from Lagrangian modelling through linearisation to discrete-time implementation, tailored specifically to 8-bit embedded hardware, complementing the optimal- and intelligent-control approaches reported elsewhere in the literature with a deterministic, computationally inexpensive alternative. Second, it delivers a quantitative experimental comparison between two empirically tuned gain configurations, demonstrating the gain-dependent boundary between successful stabilisation and a sustained oscillatory limit cycle, and thereby characterising the practical robustness margin of the controller under real hardware constraints. Third, it offers an open, reproducible platform constructed for under US$112, extending the line of low-cost didactic prototypes established by Medina Cervantes et al. (2017), Martínez Ramírez and Hernández Hernández (2025), and Yanco Melgarejo (2026) to the specific, comparatively underexplored case of the cart-mounted inverted pendulum, thereby providing an accessible laboratory resource for control engineering education.

The remainder of this paper is organized as follows. Section 2 presents the mathematical modelling of the system, the structural design and construction of the prototype, the embedded hardware and instrumentation architecture, and the PID tuning methodology. Section 3 reports and discusses the experimental results obtained under both gain configurations. Section 4 concludes the paper and outlines its implications for low-cost control engineering education.

2. Methodology

The development of the inverted pendulum on a cart was approached through a mixed theoretical-experimental methodology, structured into five sequential stages: (I) mathematical modelling; (II) structural design and construction; (III) hardware and instrumentation; (IV) controller design and discretisation; and (V) empirical tuning with experimental validation. This staged structure was not arbitrary; it follows directly from the nature of the plant itself, which is inherently unstable about its operating equilibrium. Consequently, factors that a purely analytical treatment might otherwise overlook, including measurement resolution, actuator response speed, and the mechanical disturbances arising from manufacturing tolerances, had to be anticipated from the outset and addreszed systematically at every stage, rather than treated as secondary concerns once a controller had already been derived on paper.

Each stage was therefore designed to serve a specific, complementary purpose within the overall procedure. The mathematical modelling stage establishes the theoretical foundation against which the physical prototype is subsequently measured, providing the linearized, continuous-time representation required for controller design. The structural design and construction stage translates that model into a functional electromechanical assembly capable of reproducing the predicted dynamic performance with minimal parasitic effects. The hardware and instrumentation stage closes the loop between the physical plant and the digital controller, ensuring that sensing and actuation are sufficiently fast and reliable for deterministic real-time execution. The controller design and discretisation stage transforms the continuous control law into a form suitable for implementation on resource-constrained embedded hardware. Finally, the empirical tuning stage reconciles the idealized model with the genuine behaviour of the physical system, exploiting direct experimental feedback to compensate for nonlinear effects, such as friction, backlash, and actuator dead zones, which the linear model cannot capture. Taken together, these stages constitute a coherent, reproducible pathway from first-principles dynamics to a validated, low-cost, real-time embedded controller, and they are addreszed in turn in the subsections that follow.

2.1 System modeling and analysis.

The formulation of an accurate mathematical model capable of describing the interaction among all mechanical variables of the system is essential to characterising the dynamic behaviour of the inverted pendulum on the cart. Given that the plant is nonlinear, underactuated, and exhibits strong dynamic coupling between its two degrees of freedom, the Euler-Lagrange formulation is adopted as the most suitable approach for deriving the governing equations of motion, as it obviates the need to evaluate the system's internal constraint forces explicitly. Accordingly, the geometric position of the pendulum's centre of mass within the two-dimensional plane is first established, as expreszed in the following equations:

$$x_p = x + l\sin\theta \tag{1}$$

$$y_p = l\cos\theta \tag{2}$$

Differentiating Equations (1) and (2) with respect to time, and applying the chain rule, yields the velocity components of the pendulum, expreszed in Equations (3) and (4).

$$\dot{x}_p = \dot{x} + l\dot{\theta}\sin\theta \tag{3}$$

$$\dot{y}_p = -l\dot{\theta}\cos\theta \tag{4}$$

From Equations (3) and (4), the square of the magnitude of the pendulum's linear velocity is given by: $(v_p^2 = \dot{x}_p^2 + \dot{y}_p^2)$. Through algebraic manipulation and trigonometric simplification, Equations (5) and (6) are subsequently derived.

$$v_p^2 = (\dot{x} + l\dot{\theta}\cos\theta)^2 + (-l\dot{\theta}\sin\theta)^2 \tag{5}$$

$$v_p^2 = \dot{x}^2 + 2l\dot{x}\dot{\theta}\cos\theta + l^2\dot{\theta}^2 \tag{6}$$

With the velocity of the link established, the total kinetic energy (T) of the electromechanical system can be calculated, comprising two contributions: the translational kinetic energy of the cart and the combined translational-rotational kinetic energy of the pendulum. This yields Equation (7).

$$T=\frac{1}{2}(M+m)\dot{x}^2+ml\dot{x}\dot{\theta}\cos\theta+\frac{1}{2}(I+ml^2)\dot{\theta}^2 \tag{7}$$

The total potential energy (V) of the system, which depends upon the height of the pendulum's centre of mass within the constant gravitational field (g), is expreszed in Equation (8). Combining Equations (7) and (8), the system Lagrangian is constructed as the difference between the kinetic and potential energies, L = T − V, yielding Equation (9).

$$V=mgl\cos\theta \tag{8}$$

$$L=\frac{1}{2}(M+m)\dot{x}^2+ml\dot{x}\dot{\theta}\cos\theta+\frac{1}{2}(I+ml^2)\dot{\theta}^2-mgl\cos\theta \tag{9}$$

The Euler-Lagrange equations are then applied independently to each generalized coordinate of the system, namely x and θ, as follows:

$$\frac{d}{dt}\left(\frac{\partial L}{\partial \dot{x}}\right)-\frac{\partial L}{\partial x}=F \tag{10}$$

$$\frac{d}{dt}\left(\frac{\partial L}{\partial \dot{\theta}}\right)-\frac{\partial L}{\partial \theta}=0 \tag{11}$$

For the cart coordinate (x), the procedure begins by evaluating the partial derivative of the Lagrangian with respect to the linear velocity ($\dot{x}$), yielding the following expression:

$$\frac{\partial L}{\partial \dot{x}}=(M+m)\dot{x}+ml\dot{\theta}\cos\theta \tag{12}$$

The total time derivative is then applied to Equation (12) by means of the chain rule:

$$\frac{\partial L}{\partial x}=(M+m)\ddot{x}+ml\ddot{\theta}\cos\theta-ml\dot{\theta}^2\sin\theta \tag{13}$$

Since the Lagrangian does not explicitly contain the coordinate x, the partial derivative ∂L/∂x vanishes. Substituting this result together with Equation (13) into Equation (10) yields the equation governing the cart's linear motion:

$$(M+m)\ddot{x}+ml\ddot{\theta}\cos\theta-ml\dot{\theta}^2\sin\theta=F \tag{14}$$

The partial derivative of the Lagrangian with respect to the angular velocity (θ) is calculated first:

$$\frac{\partial L}{\partial \dot{\theta}}=ml^2\dot{\theta}+ml\dot{x}\cos\theta \tag{15}$$

The total time derivative is then applied to Equation (15):

$$\frac{d}{dt}\left(\frac{\partial L}{\partial \dot{\theta}}\right)=ml^2\ddot{\theta}+ml\ddot{x}\cos\theta-ml\dot{x}\dot{\theta}\sin\theta \tag{16}$$

The partial derivative of the Lagrangian with respect to the angular coordinate (θ) is calculated next:

$$\frac{\partial L}{\partial \theta} = -ml\dot{x}\dot{\theta}\sin\theta + mgl\sin\theta \tag{17}$$

Subtracting the partial derivative with respect to the generalized coordinate from the total time derivative causes the terms involving products of velocities to cancel. The resulting expression is then divided by the common factor ml — the product of the pendulum's mass and the length of the link — to yield a more compact form suitable for analysis, furnishing the second differential equation governing the angular dynamics of the system.

Examination of the resulting equations reveals two fundamental characteristics of the system: a strong dynamic coupling between the cart's linear motion and the pendulum's angular motion, and the existence of an equilibrium point at the upper vertical position, θ = 0, which is inherently unstable.

To design a Proportional-Integral-Derivative controller, the model is linearized about this equilibrium point under the assumption of small angular deviations, whereby sin θ ≈ θ and cos θ ≈ 1. Applying these small-angle approximations yields the local linear model expreszed in Equations (18) and (19).

$$(M+m)\ddot{x} + ml\ddot{\theta} = F \tag{18}$$

$$\ddot{x} + l\ddot{\theta} - g\theta = 0 \tag{19}$$

With the local linear model established, classical control theory provides the basis for formulating a continuous Proportional-Integral-Derivative control law, which computes the control signal u(t) responsible for generating the corrective actions required to maintain the system stable about its equilibrium point.

$$u(t) = K_p e(t) + K_i \int_0^t e(\tau)d\tau + K_d \frac{de(t)}{dt} \tag{20}$$

Since the controller is implemented on a digital microcontroller, the continuous control law must be transformed into its discrete-time equivalent. This discretisation employs two standard numerical approximations: the derivative action is approximated by the backward finite-difference method, whilst the integral action is approximated using the trapezoidal rule. Applying these approximations yields a difference equation that represents the actual behaviour of the embedded software, with the control signal computed at each sampling instant expreszed in velocity form, as given in Equation (21).

$$u(k) = K_p e(k) + K_i \sum_{k=0}^{n} \frac{h(e(k)+e(k-1))}{2} + \frac{K_d(e(k)+e(k-1))}{h} \tag{21}$$

The mathematical development presented thus consolidates two principal results. First, a continuous linear model is obtained that rigorously describes the local dynamics of the mechanism; applying the Laplace transform to the linearized plant equations enables derivation of its transfer function, which may alternatively be structured as a state-space representation. Second, the difference-equation formulation of the controller demonstrates that the control law can be implemented directly in embedded hardware, confirming its practical viability.

2.2. Structural design and construction

The transition from the mathematical model to a functional electromechanical prototype is governed primarily by the design stage, during which particular care must be taken to ensure that the structure and overall assembly provide structural stability, mechanical rigidity, and unimpeded linear motion. The minimisation of mechanical vibration, induced by the actuator during operation, is likewise essential, since the system's inherently unstable dynamics are highly sensitive to external disturbances, even those of very small magnitude. Establishing a properly controlled mechanical environment therefore constitutes the first step towards a functional prototype.

To achieve the required structural precision within an economically accessible approach, the main assembly was constructed using low-density structural materials selected for their ease of machining. This choice offers an appropriate balance between lightness, mechanical rigidity, and vibration absorption, facilitating component fitting, alignment, and coupling without compromising the rigidity of the structural frame.

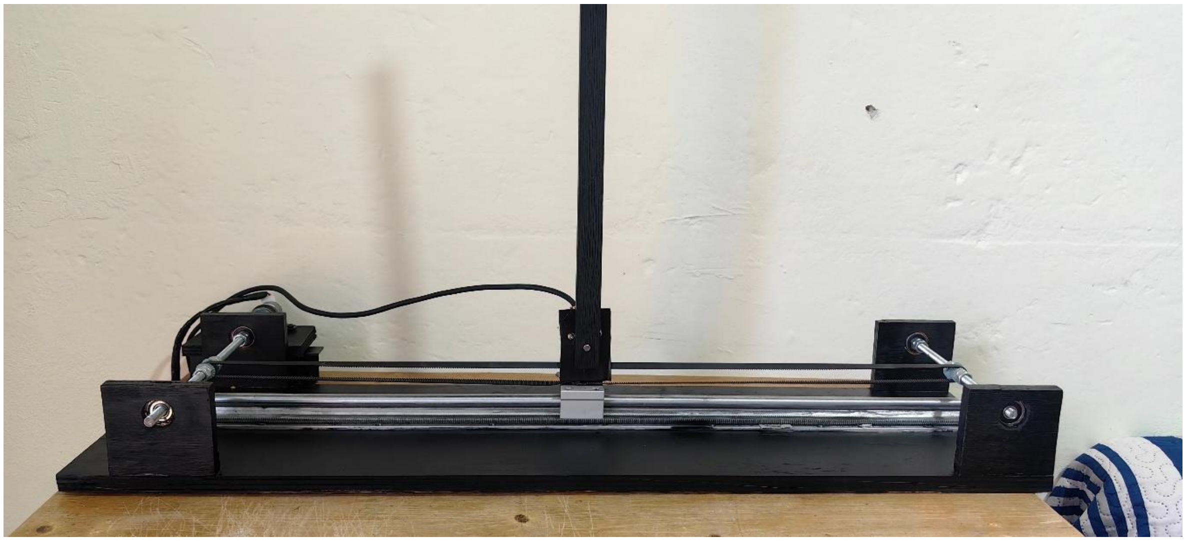

Fig. 1. Module for translation and mechanical assembly of the car.

The manufacturing process pursued two principal objectives: ensuring strictly parallel alignment of the linear guides, and minimising the mass of the mobile cart. Together, these objectives ensure the correct integration of the electromechanical components, minimise the energy losses associated with system inertia, and prevent irregularities or deformations capable of degrading the convergence of the control loop.

Fig. 2. Front view of the pendulum link and its coupling to the mobile carriage.

The translation module was designed specifically to move the cart along a rectified linear guide, with drive provided through a transmission system comprising a toothed belt and precision pulleys, directly coupled to the shaft of a direct-current motor (Fig. 1). This motor converts the pulse-width-modulated electrical signal into the mechanical force required to displace the system. The careful selection of these driving components serves two purposes: improving the actuator's response speed, and ensuring that the corrective actions computed by the control algorithm are transmitted without delay, thereby minimising dynamic lag attributable to mechanical play.

Two optical encoders were installed to record system displacements with high precision. The first encoder was directly coupled to the pendulum's rotation axis to obtain its angular position, whilst the second was integrated into the linear displacement mechanism to measure the position of the cart. Both sensors were mounted to ensure firm coupling and low mechanical resistance, thereby preserving the system's freedom of movement and reducing errors arising from friction or misalignment. Likewise, the assembly design carefully considered the distribution of the pendulum link's centre of mass and its total length (Fig. 2), with the aim of achieving predictable physical behaviour conducive to stabilisation through the PID algorithm.

2.3. Hardware and instrumentation

A hardware system was developed to experimentally validate control of the inverted pendulum on the cart, bazed on a real-time, clozed-loop architecture. The selection of processing, actuation, and instrumentation components was guided by the need to minimise latency and reading delays whilst maintaining implementation costs within an accessible range.

The choice of processing platform is a critical factor for real-time control systems, given the central importance of sampling time. Accordingly, a development platform bazed on the Arduino architecture was selected, primarily for its low cost and accessible integrated development environment (IDE), which, unlike specialized industrial controllers, offers a user-friendly interface supported by an extensive repertoire of open-source libraries. This combination renders the platform straightforward to learn and pedagogically suitable for students with only basic programming knowledge. The microcontroller supports external hardware interrupts for rapid sensor reading and provides native Pulse-Width-Modulation (PWM) channels for control of the power stage.

Cart displacement is driven by a 12 V, 600 RPM direct-current (DC) motor fitted with a reduction gearbox, selected for its favourable torque-to-inertia ratio, which provides the rapid mechanical traction required to counteract transient disturbances in an inherently unstable system. Direction and speed of this actuator are governed by an H-bridge power module (BTS7960B), operating across a voltage range of 5.5 V to 27 V DC, compatible with both 3.3 V and 5 V logic levels, and capable of delivering up to 43 A output current. This module translates the PWM signal computed by the microcontroller into the bidirectional voltage and current required for traction.

System feedback is provided by two optical encoders operating in quadrature at a resolution of 600 pulses per revolution (PPR). Their integration was designed to maximise data integrity: the first encoder, factory-coupled to the motor, registers the cart's linear displacement (x) with minimal mechanical play, whilst the second, independently mounted on the pendulum's rotation axis, measures its angular position (θ) with high fidelity. The continuous interaction between the physical variables acquired by the encoders, the algorithmic processing performed by the microcontroller, and the resulting corrective action of the H-bridge together constitute the system's integral control architecture. This signal flow, the associated data conversion, and the relationship between the hardware and the implemented mathematical blocks are illustrated schematically in the general control diagram (Fig. 3).

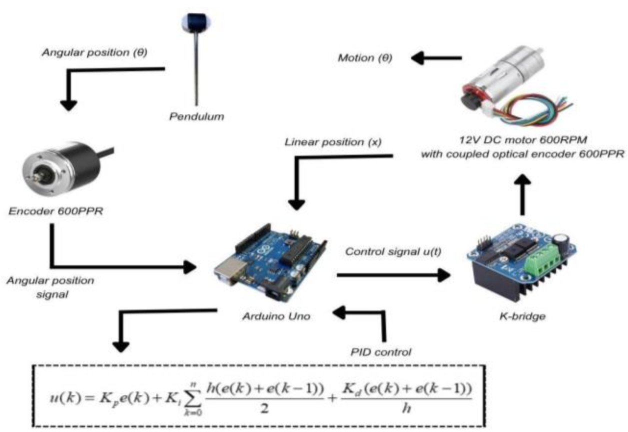

Fig. 3. General diagram of the implemented control system, showing the interaction between instrumentation, logical processing, and actuation.

As illustrated in the control system diagram (Fig. 3), the dynamic performance of the prototype depends not solely on the robustness of its components, but fundamentally on the correct digitisation of the continuous control law. The algorithmic translation of the discrete PID difference equation, whose mathematical derivation was presented previously, constitutes the logical core of the mechanism and is implemented in C/C++. This numerical processing, embedded directly within the development board, executes deterministically at each constant sampling instant: during every computational iteration, the code acquires the current position values by processing the interrupts generated by the encoders, quantifies the angular error with respect to the vertical equilibrium reference, and computes the corresponding control effort.

The interaction between physical data acquisition and logical processing is thus strictly governed by Equation (21), in which h denotes the sampling period. The following code excerpt illustrates the implementation of this discrete PID controller within the microcontroller's main loop.

```
  error = theta_ref - angulo;

// Derivative action with low-pass filter
  float derivada = error - error_prev;
  derivada_filtrada = alphaDer * derivada_filtrada + (1 - alphaDer) * derivada;

// Integral action with anti-windup saturation (h = 0.005s)
  integral += error * 0.005;
  integral = constrain(integral, -300, 300);

// PID control law
  float controlPendulo = kp * error + ki * integral + kd * derivada_filtrada;
  error_prev = error;

  float u = controlPendulo;
  if (isnan(u)) u = 0; // Safety check for NaN values

// Output control signal to the power stage
  moverMotor((int)u);
```

The propozed prototype is distinguished by its open-hardware approach, which contrasts markedly with the restrictive "black-box" environments that conceal acquisition and control processes in conventional laboratories. This design promotes deep learning by enabling students to engage directly with every layer of the system, from electronic signal conditioning to low-level programming, fostering computational autonomy independent of fixed workstations and proprietary software licences. The combination of an accessible interface, robust dynamic performance, and a modular architecture demonstrates that competitive, pedagogically superior laboratory equipment can be developed at modest cost. To quantify this achievement, a comparative table is presented below, detailing the cost breakdown of the prototype materials against the acquisition price of an equivalent commercial system.

Table 1. Price comparison of this project

Low-cost prototype				
Component	Technical Specification	Cost		
Processing unit	Arduino Uno Development Board (ATmega328P)	$450 MXN	Popular brand	+$85,000.00 MXN +$5,000.00 USD
Electromechanical actuator	12V DC Gearmotor (600 RPM) with integrated encoder	$298 MXN		
Power stage	High current H-bridge module (BTS7960B)	$150 MXN		
Angular position sensor	Quadrature rotary optical encoder (600 PPR)	$439 MXN		
Structure	MDF panels, linear guides and precision screws	$600 MXN		
Total		$1938.00 MXN $111.76 USD		

2.4. PID Controller Tuning

The PID controller was designed to maintain the pendulum close to its equilibrium position. Given the inherently unstable nature of the system, the tuning stage proved critical throughout the project, since even minor adjustments to the gains produced noticeable changes in the overall system dynamics. The tuning strategy relied on continuous feedback from the variables measured by the quadrature encoders, which provided the data required to determine both the lateral displacement of the cart and the angular position of the pendulum. The implemented control law corresponds to Equation (20), where u(t) denotes the control signal applied to the motor, e(t) the error between the desired and measured angular position of the pendulum, and Kp, Ki, and Kd the proportional, integral, and derivative gains, respectively.

Gain tuning was performed empirically through experimental trials with the physical prototype. The proportional gain was adjusted first, until a sufficiently rapid system response was achieved; the derivative gain was then introduced to minimise oscillations and ensure smooth dynamic performance; finally, the integral gain was incorporated to mitigate steady-state error without compromising the stability already attained.

When the behaviour of the physical prototype was contrasted with the theoretical mathematical model, discrepancies attributable to the real implementation became apparent. Whereas the theoretical simulation achieved a fast settling time with minimal overshoot under the calculated ideal gains, practical implementation required these values to be adjusted iteratively. This divergence is attributed to dynamics absent from the theoretical analysis, including static and dynamic friction along the cart's guide rails, dead zones in the DC motor, and the finite resolution of the encoders. Despite these nonlinearities, experimental fine-tuning enabled the system's response to converge closely towards the simulated theoretical behaviour. Evaluation of physical performance variables, namely settling time, oscillation amplitude, and angular stability, confirmed that the physical controller effectively compensates for mechanical disturbances, thereby validating the feasibility of the theoretical model under real hardware conditions, notwithstanding the limitations impozed by quantisation and PWM-bazed actuation.

3. Results and discussion

To evaluate the PID controller, distinct tests were conducted under two different tuning configurations in order to characterise the differences in the system's dynamic behaviour. The selected gains are presented in Table 2, alongside the corresponding pendulum-position response graphs. Within the control law, the proportional gain generates an immediate response to the error, increasing the system's correction speed; the integral gain mitigates any steady-state error that may arise; and the derivative gain damps the oscillations occurring about the unstable equilibrium point, smoothing the overall system dynamics. The experimental results obtained validate the contribution propozed in this work, demonstrating that the developed platform, built from open hardware and low-cost commercial components, satisfactorily reproduces the dynamic behaviour of an inverted pendulum on a cart. Furthermore, the results confirm that a classical PID controller, tuned experimentally, can stabilise the system even in the presence of phenomena not fully captured by the theoretical model, including variable friction, mechanical backlash, and actuator dead zones, thereby establishing the technical and educational viability of the proposal as a tool for teaching and experimentation in automatic control.

Table 2. Experimental tuning parameters of the PID controller.

Parameter	**Tuning 1**	**Tuning 2**
Kp	500.0	300.0
Ki	0.015	0.012
Kd	1.8	1.4

The first configuration implements an energetic control scheme, combining a relatively high proportional gain with a strong derivative action. The corresponding experimental results are presented sequentially through the angular position of the pendulum (Fig. 4) and the angular error (Fig. 5).

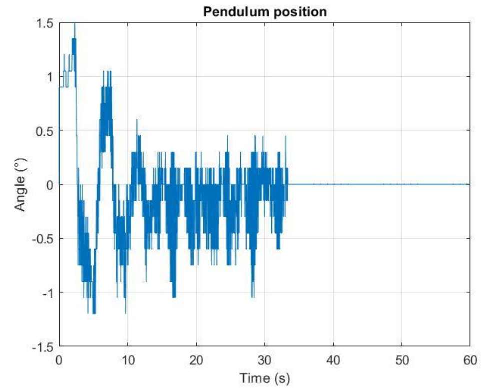

Fig. 4. Temporal response of the angular position of the pendulum under Tuning 1.

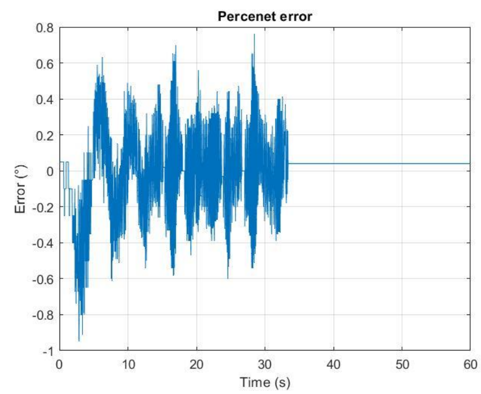

Fig. 5. Evolution of the angular error of the pendulum under Tuning 1.

Under this high proportional gain, the actuator responds rapidly to disturbance. During the first 10 seconds, coupled oscillations between the pendulum and the cart are evident, reflecting the controller's effort to balance the link. The derivative action then introduces damping that progressively attenuates these oscillations, stabilising the mechanism within approximately 33 seconds, whilst the integral action eliminates the remaining steady-state error, achieving full convergence to the desired values, as illustrated by the cart's linear position (Fig. 6) and its corresponding error (Fig. 7).

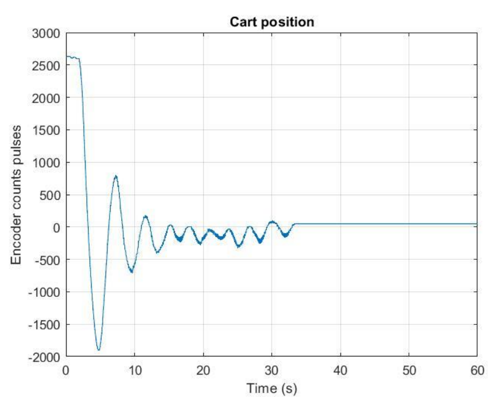

Fig. 6. Temporal response of the linear displacement of the cart under Tuning 1.

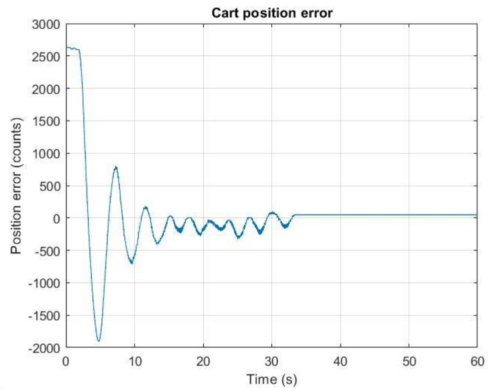

Fig. 7. Evolution of the carriage position error under Tuning 1.

This robust performance is nonetheless attained at a physical cost: the pronounced switching and variability of the PWM control signal (Fig. 8) result in increazed structural vibration and greater acoustic noise from the motor.

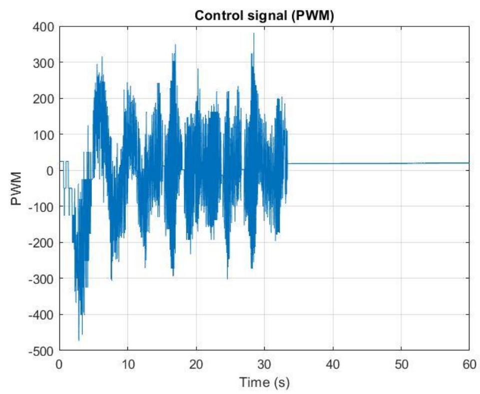

Fig. 8. Control signal (PWM) demanded to the actuator under Tuning 1.

In contrast, the second tuning configuration employed more conservative gain values, intended to reduce mechanical stress on the plant. The corresponding results present first the trajectory of the angular position (Fig. 9) and subsequently the associated error (Fig. 10).

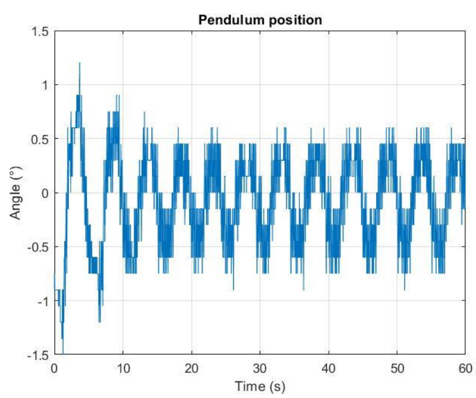

Fig. 9. Temporal response of the angular position of the pendulum under Tuning 2.

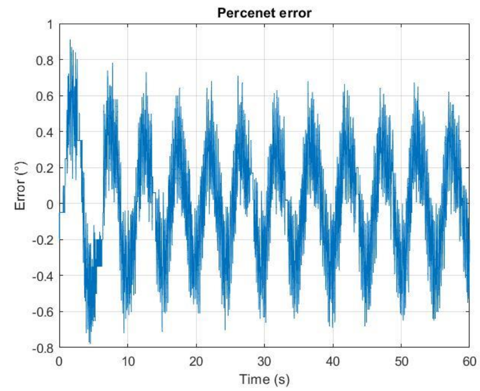

Fig. 10. Evolution of the angular error of the pendulum under Tuning 2.

Although the cart moves more smoothly during the initial transient and structural vibration decreases significantly, the analysis reveals that the controller fails to deliver sufficient corrective energy to stabilise the plant. The reduced proportional gain renders the applied horizontal force insufficient to simultaneously overcome static friction and the actuator's dead zone, driving the system into a sustained steady-state oscillatory regime, namely a limit cycle. Throughout the entire evaluation period, the pendulum's angular position, the cart's linear displacement (Fig. 11), and the corresponding position error (Fig. 12) oscillate periodically without ever converging to the desired reference values

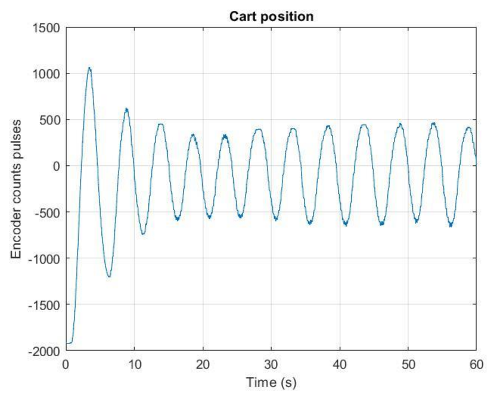

Fig. 11. Temporal response of the linear displacement of the cart under Tuning 2.

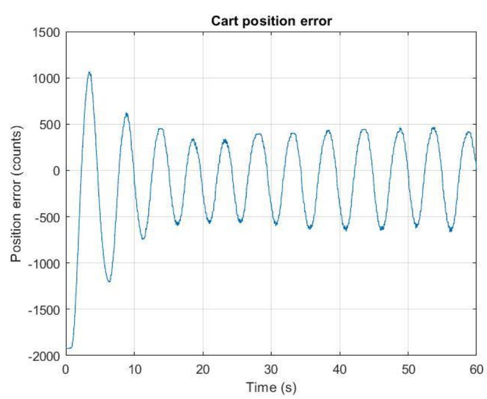

Fig. 12. Evolution of the carriage position error under Tuning 2.

These observations confirm that the system cannot be stabilized under this configuration, a conclusion corroborated by the behaviour of the control signal (Fig. 13), which exhibits a persistent oscillatory pattern, reflecting the clozed loop's inability to reach a static state owing to the insufficiency of the gains relative to the system's physical nonlinearities.

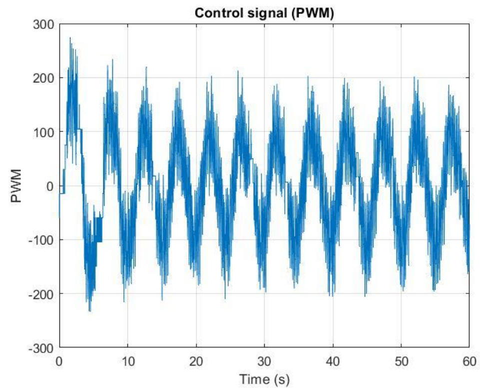

Fig. 13. Control signal (PWM) demanded to the actuator under Tuning 2.

Through direct comparison of both experiments, complex physical phenomena emerge that idealized mathematical models typically overlook: variable friction along the guide rail, small clearances within the belt transmission, and inherent delays in the motor's electromechanical response. These factors act as continuous disturbances, increasing the difficulty of stabilisation within a genuine hardware environment. Despite these practical limitations, the evidence obtained confirms the robustness of the PID controller in stabilising a strongly nonlinear system such as the inverted pendulum, provided that fine experimental tuning and proper integration of the mechanical, electronic, and computational domains are achieved. The technical and educational feasibility of the proposal is thereby validated, consolidating it as an accessible and reproducible platform for teaching and experimentation in automatic control.

4. Conclusions

This work set out to answer a specific scientific question: can a deterministic, discrete-time control law be designed, discretized, and executed in real time on an 8-bit, resource-constrained microcontroller to stabilise the nonlinear, underactuated, unstable dynamics of an inverted pendulum on a cart, using an open-hardware platform reproducible at low cost? The experimental evidence presented in this paper answers that question affirmatively, whilst also clarifying the boundary conditions under which the answer holds.

A complete methodological pathway was developed and validated, from Euler-Lagrange modelling of the coupled cart-pendulum dynamics, through linearisation about the unstable upright equilibrium, to a discrete-time Proportional-Integral-Derivative law obtained via backward-difference differentiation and trapezoidal integration. This control law was deployed on an 8-bit ATmega328P microcontroller, with interrupt-driven acquisition from two quadrature optical encoders, derivative low-pass filtering, integral anti-windup saturation, and actuation through an H-bridge-driven direct-current motor. The platform was constructed for under US$112, confirming that deterministic real-time control execution is achievable on genuinely resource-constrained embedded hardware, without recourse to specialized processing units.

The hypothesis that a classically tuned discrete PID controller could stabilise the system despite unmodelled nonlinearities was confirmed, but only within a defined operating envelope. Under the first, more aggressive gain configuration (Kp = 500, Ki = 0.015, Kd = 1.8), the controller successfully stabilized the pendulum within approximately 33 seconds, demonstrating that sufficiently energetic corrective action can overcome static and dynamic friction, mechanical backlash, and actuator dead zones that are absent from the idealized linear model. Under the second, more conservative configuration (Kp = 300, Ki = 0.012, Kd = 1.4), the applied horizontal force proved insufficient to overcome these same nonlinearities, and the system settled into a sustained oscillatory limit cycle rather than converging to the reference. This contrast is itself a substantive result: it quantifies the gain-dependent stability margin of the physical plant and demonstrates, empirically, that the gap between simulated and real behaviour is not merely qualitative but has a measurable threshold.

These findings directly support the three contributions claimed in the Introduction. First, the reproducible methodological pathway, from Lagrangian derivation to discrete embedded implementation, offers a deterministic, computationally inexpensive alternative to the optimal and intelligent control architectures reported elsewhere, including LQR-bazed schemes (Juárez-Lora & Hernández-Pérez, 2022; Hernández-Pérez & Gutiérrez, 2024) and fuzzy-PID approaches with state estimation (Alvarado-Hernández et al., 2025; Narciso et al., 2023). Second, the quantitative comparison between the two tuning configurations characterises the practical robustness margin of the controller under genuine hardware constraints, a dimension that purely simulated studies cannot capture. Third, the resulting open-hardware platform extends the established line of low-cost didactic prototypes, including the Furuta pendulum work of Medina Cervantes et al. (2017) and Martínez Ramírez and Hernández Hernández (2025), and the Arduino-bazed aerodynamic pendulum of Yanco Melgarejo (2026), to the comparatively underexplored cart-mounted configuration, providing an accessible and reproducible laboratory resource for control engineering education.

The development of this prototype therefore integrates mathematical modelling, electronics, embedded programming, and automatic control into a single, low-cost teaching platform, reaffirming the inverted pendulum as a demanding and pedagogically valuable testbed for the study of nonlinear, underactuated dynamics. Unlike approaches that remain confined to simulation or rely on ready-to-use commercial equipment, the platform reported here was built from open hardware and validated under real operating conditions, which is not a guaranteed outcome when moving beyond the simulator. It is documented in sufficient detail to be replicated by other laboratories without the budgetary burden of commercial alternatives, allowing students to test classical control strategies directly on physical hardware.

Future work should exploit this same open-hardware platform to evaluate, under identical physical constraints, the optimal and intelligent control strategies reviewed in the Introduction, such as LQR and fuzzy-PID schemes, thereby establishing a direct, hardware-validated comparison against the classical discrete PID baseline characterized in this study.

References

Alvarado-Hernandez, J.-R., Pérez-Perea, J.-E., Martínez-De La Cruz, A., Domínguez-Ortega, O., Ramos-Gálvez, E.-M., Ordaz, P., & Ordaz Oliver, M. O. (2025). Fuzzy-PID control with state estimation for the regulation of an aero-pendulum system. In *2025 11th International Conference on Mechatronics and Robotics Engineering (ICMRE)* (pp. 187–192). IEEE. https://doi.org/10.1109/ICMRE64970.2025.10976289

Aracil, J., & Gordillo, F. (2005). El péndulo invertido: Un desafío para el control no lineal. *Revista Iberoamericana de Automática e Informática Industrial, 2*(2), 8–19. https://doi.org/10.4995/riai.v2i2.10501

Hernández Pérez, J., Gutiérrez Moreno, E., Ordaz Oliver, J. P., & Ordaz Oliver, M. O. (2024). LQR-based control with gravity compensation for a wind turbine pendulum system. *International Journal of Combinatorial Optimization Problems and Informatics, 15*(5), 161–180. https://doi.org/10.61467/2007.1558.2024.v15i5.428

Juárez-Lora, J. A., Sossa Azuela, J. H., Ponce-Ponce, V. H., Rubio-Espino, E., & Barrón Fernández, R. (2022). Spiking neural network implementation of LQR control on underactuated system. *International Journal of Combinatorial Optimization Problems and Informatics, 13*(4), 36–46. https://doi.org/10.61467/2007.1558.2022.v13i4.320

Martínez Ramírez, E., Diaz Ledezma, M. A., López Portillo Zuarth, D., Vicente Ortiz, A. Y., Mera Sánchez, N. R., Ordaz Oliver, M. O., & Espejel Rivera, M. A. (2025). Model of a low-cost educational prototype of the Furuta pendulum. *International Journal of Combinatorial Optimization Problems and Informatics, 16*(4), 61–78. https://doi.org/10.61467/2007.1558.2025.v16i4.1133

Medina Cervantes, J., Gallardo Sánchez, J. E., Villafuerte Díaz, R., & Mejía Sánchez, E. (2017). Desarrollo de un péndulo de Furuta. *Revista Electrónica sobre Tecnología, Educación y Sociedad, 4*(7). https://www.ctes.org.mx/index.php/ctes/article/view/619

Morales-Narciso, L.-M., Mendoza-Reyes, I., Romero-Flores, R.-N., Martínez-Ramírez, W.-D.-J., Calderon-Lopez, J.-V., López-García, A.-M., Flores-Alvarez, M.-Á., Ordaz-Oliver, M.-O., & Ordaz, P. (2023). Design, construction and control of a seesaw system driven with a thrust propeller. In *2023 XXV Robotics Mexican Congress (COMRob)* (pp. 122–127). IEEE. https://doi.org/10.1109/COMRob60035.2023.10349707

Pérez Garcia, B., Monroy Mendoza, M. F., Ramírez Alvarado, J. J., Gutiérrez Paredes, J. A., Melgarejo Tolentino, Y., Hernández Pérez, J., & Gutiérrez Moreno, E. (2026). Closed-loop control and sensor noise reduction in a low-cost aerodynamic pendulum using digital PID and Kalman filtering on Arduino Mega. *International Journal of Combinatorial Optimization Problems and Informatics, 17*(1), 34–47. https://doi.org/10.61467/2007.1558.2026.v17i1.1137

Ronquillo Lomeli, G. (2025). Nonlinear systems modeling using polynomial neural networks: Comparison. *International Journal of Combinatorial Optimization Problems and Informatics, 16*(4), 259–272. https://doi.org/10.61467/2007.1558.2025.v16i4.936